

NATIONAL AERONAUTICS AND SPACE ADMINISTRATION

Technical Report 32-1134

*Balanced Filters for the Analysis of
Al, Si, K, Ca, Fe, and Ni*

J. A. Dunne

N. L. Nickle

GPO PRICE \$ _____

CFSTI PRICE(S) \$ _____

Hard copy (HC) \$ 3.00

Microfiche (MF) \$.65

ff 653 July 65

**JET PROPULSION LABORATORY
CALIFORNIA INSTITUTE OF TECHNOLOGY
PASADENA, CALIFORNIA**

August 1, 1967

N67-33229

(ACCESSION NUMBER)

(THRU)

(PAGES)

(CODE)

(NASA CR OR TMX OR AD NUMBER)

(CATEGORY)

NATIONAL AERONAUTICS AND SPACE ADMINISTRATION

Technical Report 32-1134

*Balanced Filters for the Analysis of
Al, Si, K, Ca, Fe, and Ni*

J. A. Dunne

N. L. Nickle

Approved by:



Robert J. Mackin, Jr., Manager
Lunar and Planetary Sciences Section

**JET PROPULSION LABORATORY
CALIFORNIA INSTITUTE OF TECHNOLOGY
PASADENA, CALIFORNIA**

August 1, 1967

TECHNICAL REPORT 32-1134

Copyright © 1967
Jet Propulsion Laboratory
California Institute of Technology

Prepared Under Contract No. NAS 7-100
National Aeronautics & Space Administration

PRECEDING PAGE BLANK NOT FILMED.

Acknowledgment

The assistance of Mr. Rex A. Shields of the Radiation Physics Group at JPL, who designed and built the flow proportional detector used in the breadboard analyzer, is gratefully acknowledged.

PRECEDING PAGE BLANK NOT FILMED.

PRECEDING PAGE BLANK NOT FILMED

Contents

I. Introduction	1
II. Apparatus and Technique	1
III. The Balanced Filters	3
IV. Analytical Data	4
V. Conclusions	6
References	7

Table

1. Pass and absorption filter data	2
--	---

Figures

1. Chemical and mineralogical analyses of two rock samples	2
2. Diagrammatic representation of Norelco vacuum spectrometer showing the position of the filter wheel	3
3. Diagrammatic representation of breadboard instrument	3
4. Ratio of transmitted intensities as a function of wavelength	3
5. Si standard pass filter spectra at 10- and 25-kv potentials	4
6. Analytical data on standard samples	5
7. Relationships between the mass absorption coefficient and Be window transmission for the elements analyzed	5
8. Summary of rock specimen analyses	6
9. Ca filter pair transmission spectra for a standard sample and rock specimen	6

PRECEDING PAGE BLANK NOT FILMED

Abstract

The design of auxiliary instrumentation for the X-ray fluorescence analysis of the elements Al, Si, K, Ca, Fe, and Ni was the result of one phase of research in a program to develop an instrument for remote X-ray diffraction analysis of lunar and planetary surface materials. The performance of balanced filters as dispersive elements is being evaluated for comparison with that of the electronic dispersion (pulse height analysis) technique.

Balanced Filters for the Analysis of Al, Si, K, Ca, Fe, and Ni

I. Introduction

This work is a portion of the Lunar and Planetary X-Ray Diffraction Program at JPL, which is devoted to the development of instrumentation for the mineralogical analysis of lunar and planetary surface material.

A miniaturized X-ray diffractometer, developed by William Parrish of Philips Laboratories, has been extensively tested at JPL (Refs. 1 and 2) with very satisfactory results. It has become apparent (Refs. 3 and 4) that a relatively modest increase in complexity of the instrument (i.e., the addition of a second gas proportional detector), would increase the analytical value of this diffractometer by providing some X-ray fluorescence capability. Owing to the limited energy resolution of gas proportional detectors, balanced filters have been proposed (Refs. 5, 6, 7, and 8) that would provide discrimination between the fluorescence radiations of adjacent elements. This report describes the application of balanced filters to the analyses of certain major elemental constituents of terrestrial igneous rocks and stone meteorites.

Data on the chemical composition of the analyzed sample will be useful in two principal ways: (1) they will

assist in the interpretation of the diffraction diagram, and (2) they will provide some compositional information even on amorphous samples such as igneous or shock-produced glasses. Taken alone, however, determinations of the elements Al, Si, K, Ca, Fe, and Ni are of limited interpretive value. The alpha-particle scattering device that will be employed in the *Surveyor* Project (Refs. 9 and 10) can provide analyses on the more diagnostic set of elements O, Na, Mg, and Si. In any event, diffraction data are of unquestionably greater value than chemical information in the interpretation of the petrology and thermal history of the analyzed sample. This point is illustrated in Fig. 1, where chemical and mineralogical compositions are given for two rocks that have undergone significantly different degrees of thermal metamorphism (Ref. 11). The record of these events is clearly contained in the mineralogical rather than the chemical data.

II. Apparatus and Technique

Table 1 lists the pass and absorption filters used for the analyses reported here, and the compounds from which they were made. With the exception of the metal foil filters, all of the filters consist of dried slurries

Table 1. Pass and absorption filter data

Element	Wavelength, Å	Pass filter	Absorbing filter	Number of channels	Counts/min/channel/wt %
Al	8.34	Al ^a (4.53) ^b	Mg ^a (6.36)	35	30
Si	7.13	Si (5.45)	Al ^a (8.15)	44	16
K	3.74	KHCO ₃ (11.4)	S (19.8)	33	1800
Ca	3.36	CaCO ₃ (14.4)	KHCO ₃ (16.4)	41	540
Fe	1.94	MnO ₂ (26.2)	Cr ₂ O ₃ (29.6)	43	2100
Ni	1.66	Co (32.5)	Fe (36)	43	600

^aMetal foil filters.
^bNumbers in parentheses are the element-equivalent filter area density in mg/cm², measured at the balancing wavelength.

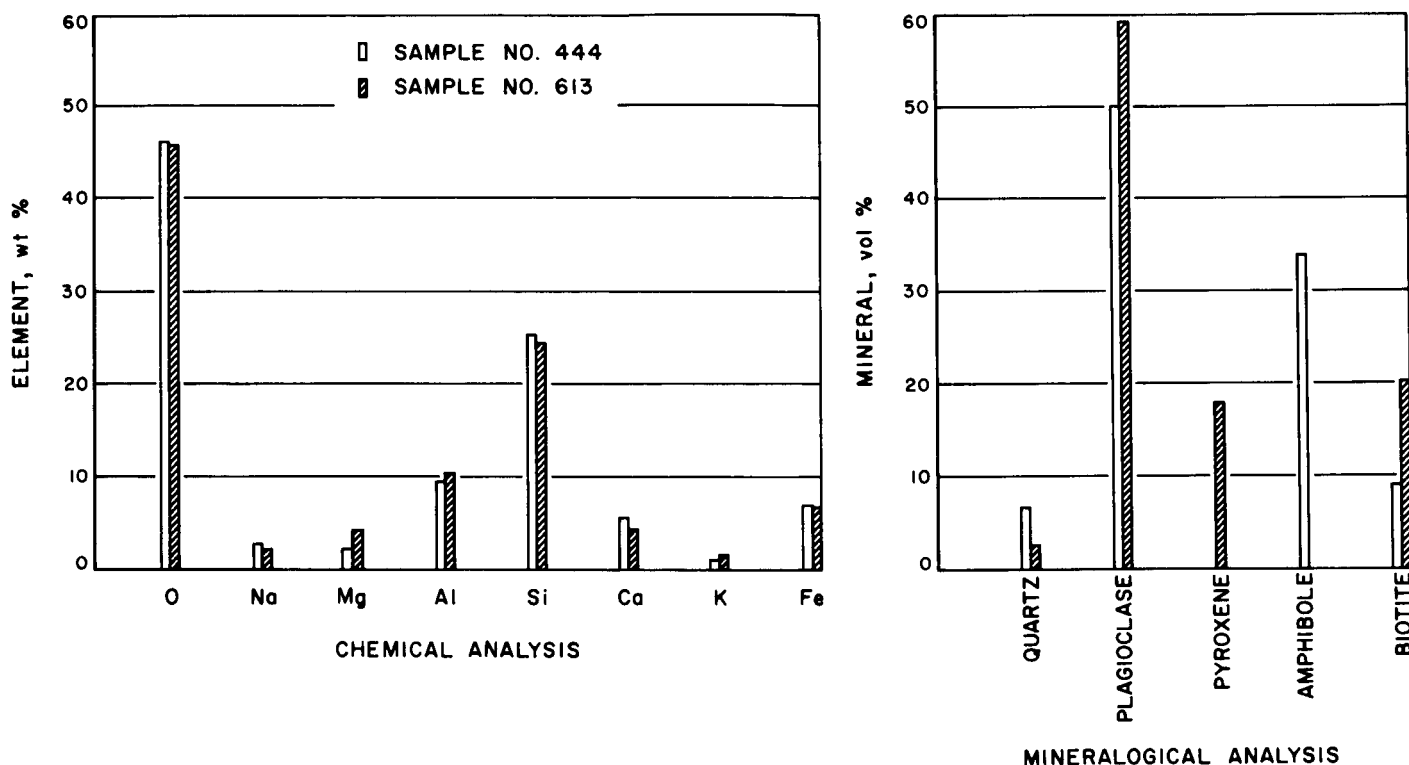


Fig. 1. Chemical and mineralogical analyses of two rock samples

of the powdered compounds and polystyrene. Area densities were adjusted by varying the (toluene) solvent-to-polystyrene ratio of the slurries. The filters were cast on glass microscopic slides, and the solvent allowed to evaporate in air. Typical drying time was a few minutes. Transmissions were measured using a standard Norelco vacuum spectrometer with a filter-holding wheel mounted on the entrance collimator (Fig. 2). Analyses were conducted with the breadboard instrument sketched in Fig. 3. The motor-driven, filter-holding wheel and the

analyzing flow proportional detector were mounted on the frame of a prototype model of the lunar X-ray diffractometer (Ref. 1). The circular, 1-cm-diameter detector window was a 1/4-mil, aluminized mylar film supported on a 200-mesh, photo-etched Ni grid; the counting gas was P-10 (90% Ar, 10% methane). The miniaturized X-ray tube (Ref. 1) was operated at 25 kv and 1 ma for most analyses, with the exceptions discussed below. The total flux at the anode has been estimated to be approximately 5×10^{12} Cu K α photons/sec,

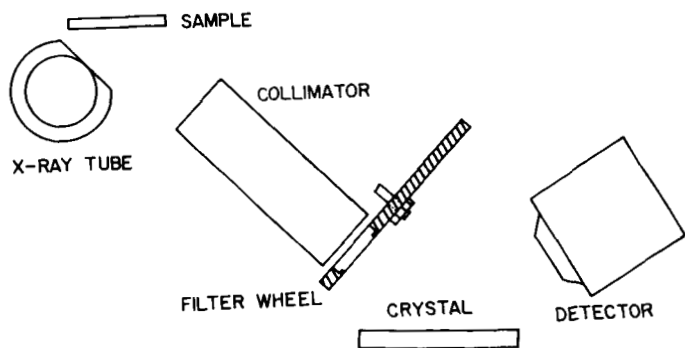


Fig. 2. Diagrammatic representation of Norelco vacuum spectrometer showing the position of the filter wheel

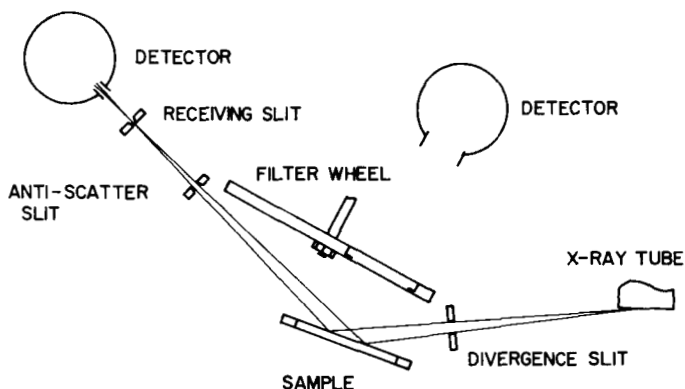


Fig. 3. Diagrammatic representation of breadboard instrument

with roughly an equivalent quantity of continuum (Bremsstrahlungen) (Ref. 12). The severe optical aperturing required for the diffraction geometry reduces this to approximately 2×10^8 Cu $K\alpha$ photons/sec at the sample surface. The analyzing electronics consisted of a Nuclear Data Model 110, 128-channel pulse-height analyzer, and a Tennelec Model 100B preamplifier modified to produce a pulse decay time constant of 1.6 μ sec.

III. The Balanced Filters

The calculated ratios of transmitted intensities ($I_{pass}/I_{absorption}$) as a function of wavelength for the filters listed in Table 1 are plotted in Fig. 4. The calculations were made assuming filters of the element having the area densities measured for the actual filters at the balancing wavelength. Figure 4, then, shows the theoretical efficiency with which properly balanced pure element filter pairs, characterized by the area densities given in

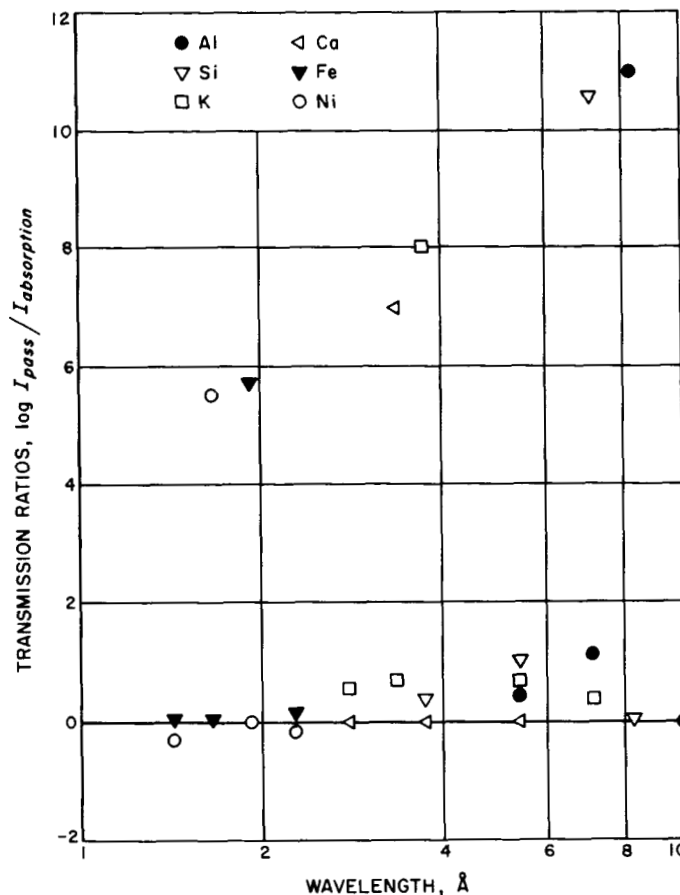


Fig. 4. Ratio of transmitted intensities as a function of wavelength

Table 1, can isolate the required lines from polychromatic spectra. The loss in contrast in the region between respective absorption edges with increasing atomic number (indicated in Fig. 4) reflects the corresponding decrease in the difference between the mass absorption coefficients of the pass and absorption filters in the region between the absorption edges. The transmission ratios shown in Fig. 4 are not realistic for the filters used in this study, because, with the exception of the Al and Mg foils, the filters were not composed of the element alone. Absorption filter transmissions for the desired wavelength, however, were too small to measure.

In any event, the transmission contrast between the pass and absorbing filters in the region between their absorption edges is not the limiting factor in the analyses, particularly in the analyses of the lighter elements. Both filters, however evenly matched, transmit large quantities of radiation on both sides of the high contrast region. The inherently higher contrast at long analytical

wavelengths relative to the contrast at shorter wavelengths is more than offset by this effect. The high transmission of the lighter element filters for wavelengths in the region of Cu $K\alpha$ presents a serious difficulty in Al and Si analyses using the Cu target X-ray source. This is illustrated in Fig. 5, which shows spectra obtained from a Si standard at 25 and 10 kv X-ray potentials. The sample contains 2.5 wt % Si in a matrix of approximately 50 wt % Methocel¹ and 50 wt % Fe_2O_3 . Both of the spectra shown in Fig. 5 were taken through the Si pass filter. The beam current was adjusted so that the total intensity transmitted through the filter was the same for both spectra. The higher energy component, principally Fe $K\alpha$, which is very efficiently excited by Cu characteristic radiation, is virtually unattenuated by the Si filter. Because the Cu and Si absorption edges are at 9 and 1.8 keV respectively, the higher (25 kv) accelerating potential favors the excitation of Fe over that of Si. As a result, the ratio of Si to Fe radiation in the transmitted spectrum is much lower at 25 kv than at 10 kv. The problem is complicated by the fact that the distortion-free operating region of gas proportional detectors is limited to rather low ($\leq 10^4$ counts/sec) total

¹An hydroxypropyl methylcellulose manufactured by Dow Chemical Co.

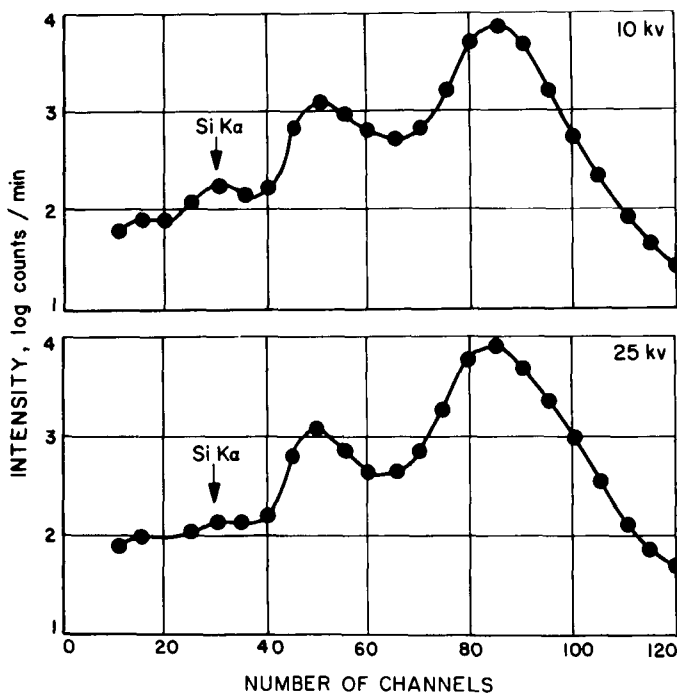


Fig. 5. Si standard pass filter spectra at 10- and 25-kv potentials

counting rates. Therefore, the ratio of the desired element wavelength to other wavelengths in the transmitted spectrum fundamentally limits the observable contrast between that element's pass and absorption filters. Obviously, this ratio cannot be improved by heavier filtration where the spectrum contains interfering wavelengths for which the pass filter's mass absorption coefficients are lower than that for the desired wavelength. For this reason, the data for Si in the standard samples were obtained at 10 kv, and that for Al at 15 kv.

The ratio of Si to Fe in the observed spectrum can be markedly improved by changing the counting gas from Ar to Ne. If the gas pressure and detector path length were adjusted to produce 95% absorption of Si $K\alpha$, the absorption for Fe $K\alpha$ would be about 60% using Ar, but only 7-1/2% under the same conditions using Ne. In this way, the Si/Fe spectral ratio could be improved by a factor of about eight; unfortunately, Ca and K sensitivities would drop off by a factor of between 2-1/2 and 3. However, the data in Section IV on Ar escape peak interference with Ca and K analyses also suggest a change in counting gas.

IV. Analytical Data

Data were collected on artificial standard samples and some analyzed rock specimens using the breadboard apparatus sketched in Fig. 3. The standards were mixtures of the elements or their compounds with a matrix that consisted of 50 wt % each of powdered Si and Methocel. The matrix of the Si standards discussed in Section III was half Methocel and half Fe_2O_3 . The standards were pelletized in a hydraulic press at 4×10^4 psi. Results are given in Fig. 6, and are summarized in Table 1 in terms of counts/min/channel/wt %. The relative sensitivities indicated in Fig. 6 and Table 1 can be compared with the relationships plotted in Fig. 7, which shows the mass absorption coefficient of the analyzed elements for Cu $K\alpha$, as well as the 0.002-in.-thick X-ray tube Be window transmission for the wavelengths at their respective absorption edges. The importance of selecting a source with a strong line spectrum in the immediate vicinity (on the short wavelength side) of the desired element's absorption edge is evident here, as has been emphasized repeatedly by Henke (Ref. 13) and others. The sensitivity of the Ni analysis, which is high relative to that of the analyses of Si and Al, results from two factors that are in addition to the contrast discussed for Si in Section III: (1) the continuum peak, which

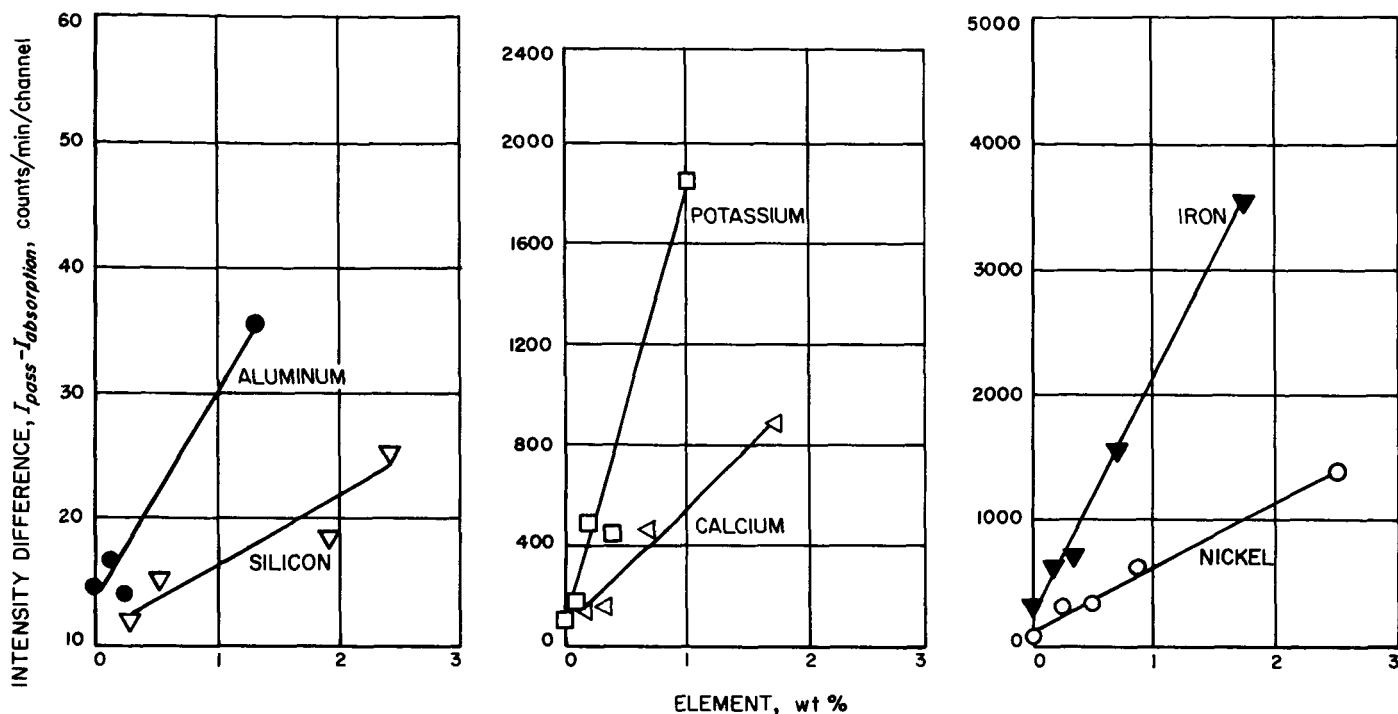


Fig. 6. Analytical data on standard samples

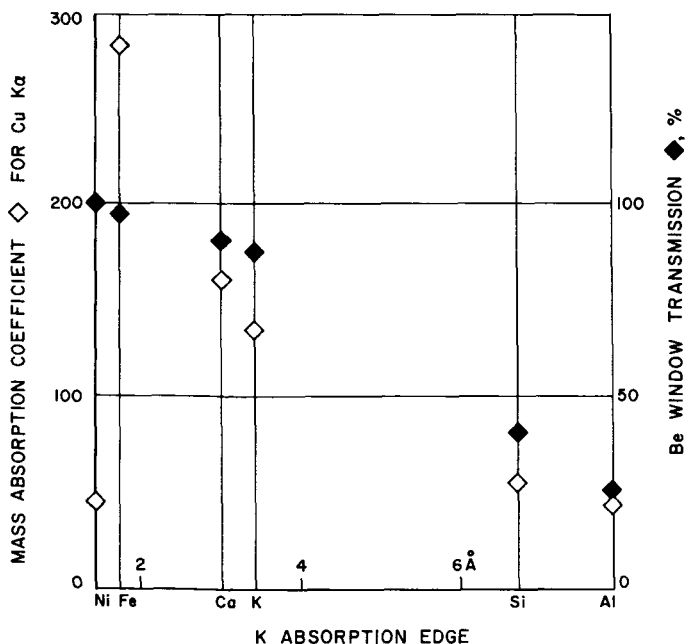


Fig. 7. Relationships between the mass absorption coefficient and Be window transmission for the elements analyzed

transmission for Ni is about twice as high as that for Si and Al.

The rock specimens analyzed were obtained from A. A. Loomis of the Planetology Group at JPL. The rocks are metavolcanics from the California Sierra, with a range of SiO₂ content between 52 and 68 wt % (Ref. 11). The data obtained from these specimens are summarized in Fig. 8. The same number of channels listed in Table 1 were used in the analyses. The data for Si as well as those for Al were taken at 15 kv in this case because none of the specimens were as rich in iron (35 wt %) as were the Si standards. The count accumulation time for each of the elements except Al was 1 min/filter. Aluminum counts were accumulated at 2 min/filter. The total counting rates were held below 5×10^3 counts/sec in every case. Nickel analyses were not attempted because the analysis of this element is desirable only where meteoritic material is encountered. While such an occurrence is not unlikely on the surfaces of the Moon or Mars, terrestrial igneous rocks are typically poor in Ni.

Ca and K analyses were complicated by escape peak interferences. Fe K α is 2.7 and 3.1 keV more energetic than Ca and K radiations, respectively. Because the Ar K absorption energy is 3.2 keV, a sample rich in Fe will present interference problems in Ca and K analyses

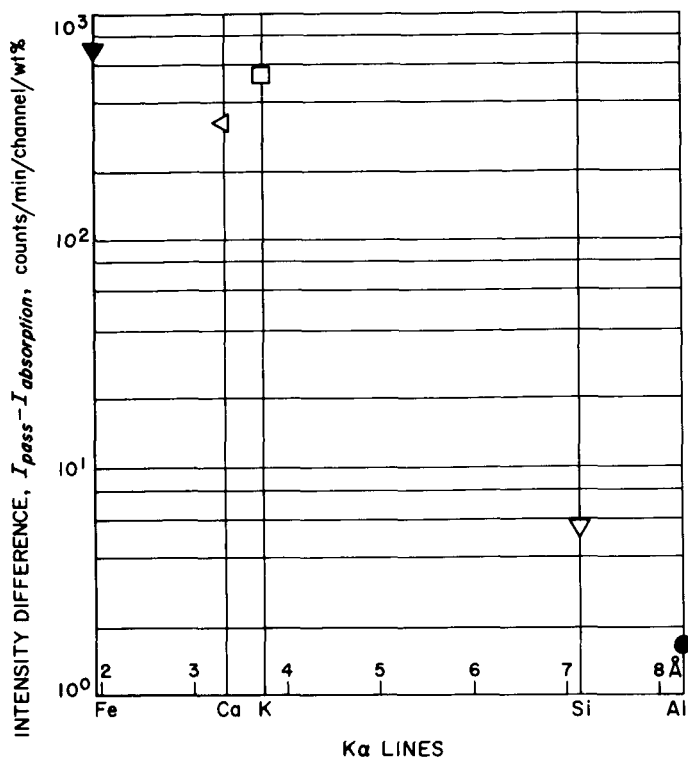


Fig. 8. Summary of rock specimen analyses

where Ar counting gas is used. This is shown in Fig. 9, which shows the Ca filter pair transmission spectra for a standard sample (1.75 wt % Ca, no Fe) and rock sample no. 36 (2.01 wt % Ca, 2.64 wt % Fe). The Fe $K\alpha$ escape peak accounts for more than 60% of the interference shown in Fig. 9, the remainder being K $K\alpha$ fluorescence radiation from the sample.

Escape peak interferences can be avoided in most cases by proper selection of the counting gas. In the analyses of Ca and K in Fe-rich samples, the use of Xe gas would solve the problem. However, the Xe (L_{III}) escape peak from Fe $K\alpha$ radiation falls in the middle of the Al-Si energy region. Neon, on the other hand, would produce little interference because its K absorption energy is only 874 eV, making its escape peak due to Fe $K\alpha$ readily resolvable from Ca and K. The Ne-K $K\alpha$ escape peak occurs at 2.43 keV, and therefore partially overlaps the Si $K\alpha$ (1.74 keV) energy distribution. The absorption of Ne for K $K\alpha$ is, however, considerably less than that of Ar or Xe for Fe, and the resolution of its K $K\alpha$ escape peak from Si is better than that of the Ar-Fe $K\alpha$ peak

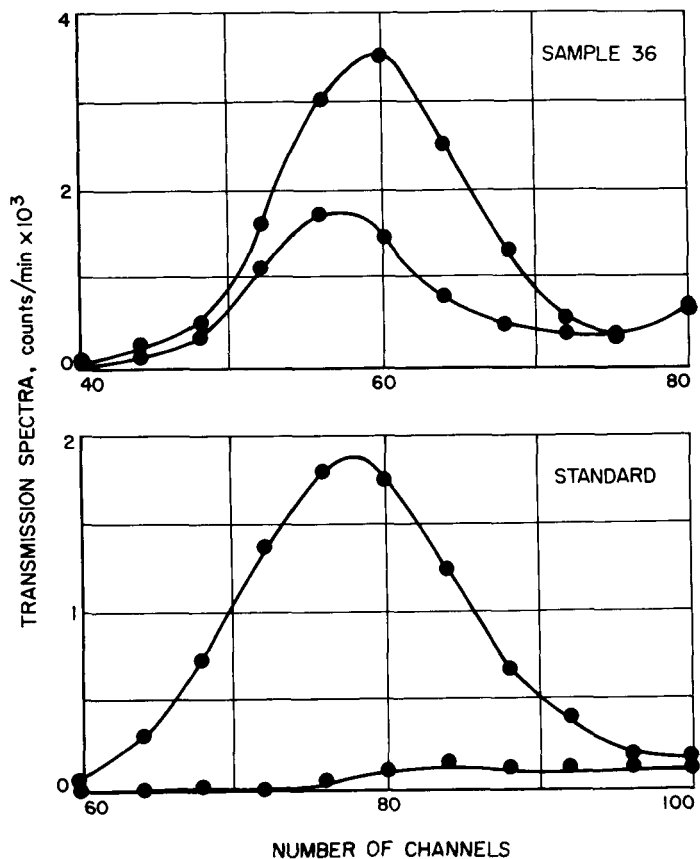


Fig. 9. Ca filter pair transmission spectra for a standard sample and rock specimen

from Ca and K, or the Xe (L_{III})-K $K\alpha$ peak from Al and Si. The advantages of Ne with regard to the Si/Fe ratio of the observed spectrum have been discussed in Section III.

V. Conclusions

The balanced filter technique offers a satisfactory method of dispersion in the atomic number region studied. The primary X-ray flux available at the sample surface is more than adequate for X-ray fluorescence analysis of the elements Al, Si, K, Ca, Fe, and Ni when they exist in the sample in amounts greater than 1 wt %. The Cu target X-ray tube is, however, far from optimum for the analysis of Al and Si. The relatively poor performance of Ar counting gas in the analyses of Si and Al, combined with escape peak interference in Ca and K analyses, suggest the use of Ne rather than Ar as the counting gas in this particular application.

References

1. Speed, R. C., Nash, D. B., and Nickle, N. L., "A Lunar X-Ray Diffraction Experiment," in *Advances in X-Ray Analysis*, Vol. 8, pp. 400-419. Edited by W. Mueller, G. Mallett, and M. Fay. Plenum Press, New York, 1965.
2. *Lunar and Planetary X-Ray Diffraction Program, Progress Report of Research and Instrument Development, July 1964 to March 1965*, Technical Memorandum 33-218. Edited by R. C. Speed, J. A. Dunne, and D. B. Nash. Jet Propulsion Laboratory, Pasadena, Calif., June 1, 1965.
3. Dunne, J. A., "Total Iron Analysis by Ancillary Non-Dispersive X-Ray Fluorescence Instrumentation," in *Lunar and Planetary X-Ray Diffraction Program, Progress Report of Research and Instrument Development, July 1964 to March 1965*, Technical Memorandum 33-218. Edited by R. C. Speed, J. A. Dunne, and D. B. Nash. Jet Propulsion Laboratory, Pasadena, Calif., June 1, 1965.
4. Das Gupta, K., et al., "A Combined Focusing X-Ray Diffractometer and Non-Dispersive X-Ray Spectrometer for Lunar and Planetary Analysis," in *Advances in X-Ray Analysis*, Vol. 9, pp. 221-243. Edited by W. Mueller, G. Mallett, and M. Fay. Plenum Press, New York, 1965.
5. Ross, P. A., "A New Method of Spectroscopy for Faint Radiations," *J. Opt. Soc. Am.*, Vol. 16, No. 6, pp. 433-437, June 1928.
6. Cameron, J. F., and Rhodes, J. R., "Filters for Energy Selection in Radioisotope X-Ray Techniques," in *The Encyclopedia of X-Rays and Gamma Rays*, pp. 387-392. Edited by G. L. Clark. Reinhold Publishing Co., New York, 1963.
7. Dunne, J. A., "Application of Ross Filter to the Non-Dispersive X-Ray Analysis of Aluminum and Silicon," *Norelco Reporter*, Vol. 8, pp. 21-24, 1966.
8. Rhodes, J. R., "Radioisotope X-Ray Spectrometry," *The Analyst*, Vol. 91, No. 1088, pp. 683-699, Nov. 1966.
9. Loomis, A. A., "Interpretation of Lunar Alpha-Scattering Data," *J. Geophys. Res.*, Vol. 70, No. 16, pp. 3841-3849, Aug. 15, 1965.
10. Patterson, J. M., Turkevitch, A., and Franzgrote, E., "Chemical Analysis of Surfaces Using Alpha Particles," *J. Geophys. Res.*, Vol. 70, No. 6, pp. 1311-1327, Mar. 15, 1965.
11. Loomis, A. A., "Contact Metamorphic Reactions and Processes in the Mt. Tallac Roof Remnant, Sierra Nevada, California," *J. Petrol.*, Vol. 7, pp. 221-245, 1966.
12. Dunne, J. A., "Preliminary Investigation of the Feasibility of a Radioisotope X-Ray Source," in *Lunar and Planetary X-Ray Diffraction Program, Progress Report of Research and Instrument Development, July 1964 to March 1965*, Technical Memorandum 33-218. Edited by R. C. Speed, J. A. Dunne, and D. B. Nash. Jet Propulsion Laboratory, Pasadena, Calif., June 1, 1965.
13. Henke, B. L., "Sodium and Magnesium Fluorescence Analysis - Part I: Method," in *Advances in X-Ray Analysis*, Vol. 6, pp. 361-376. Edited by W. Mueller, G. Mallett, and M. Fay. Plenum Press, New York, 1965.